Numerical Simulation on Intergranular Microcracks in Interconnect Lines Due to Surface Diffusion Induced by Stress-, Electro- and Thermo-migration

ZHOU Linyong, *HUANG Peizhen**

State Key Laboratory of Mechanics and Control of Mechanical Structures,
Nanjing University of Aeronautics and Astronautics, Nanjing 210016, P. R. China

(Received 20 December 2018; revised 5 August 2019; accepted 25 September 2019)

Abstract: Based on the weak formulation for combined surface diffusion and evaporation-condensation, a governing equation of the finite element is derived for simulating the evolution of intergranular microcracks in copper interconnects induced simultaneously by stressmigration, electromigration and thermomigration. Unlike previously published works, the effect of thermomigration is considered. The results show that thermomigration can contribute to the microcrack splitting and accelerate the drifting process along the direction of the electric field. The evolution of the intergranular microcracks depends on the mechanical stress field, the temperature gradient field, the electric field, the initial aspect ratio and the linewidth. And there exists a critical electric field χ_c, a critical stress field $\hat{\sigma}_c$, a critical aspect ratio β_c and a critical linewidth $\hat{h}_c$. When $\hat{\sigma} \geqslant \hat{\sigma}_c$, $\chi \geqslant \chi_c$, $\beta \geqslant \beta_c$ or $\hat{h} \leqslant \hat{h}_c$, the intergranular microcrack will split into two or three small intergranular microcracks. Otherwise, the microcrack will evolve into a stable shape as it migrates along the interconnect line. The critical stress field, the critical electric field and the critical aspect ratio decrease with a decrease in the linewidth, and the critical linewidth increases with an increase in the electric field and the aspect ratio. The increase of the stress field, the electric field or the aspect ratio and the decrease of the linewidth are not only beneficial for the intergranular microcrack to split but also accelerate the microcrack splitting process.

Key words: stressmigration; electromigration; thermomigration; surface diffusion; finite element method; intergranular microcrack

CLC number: TN925 **Document code**: A **Article ID**: 1005-1120(2019)06-1004-14

0 Introduction

There is a long-standing interest in the reliability of interconnect lines. The interest originates to a large extent from the fact that interconnect lines are abundantly used in the ongoing miniaturization of microelectronic circuits and microelectromechanical systems. Interconnect lines have bamboo grain structure with dimensions in the submicron range and the material within the interconnect line is subjected to severe mechanical and electric loading. In addition, interconnect lines inevitably exist some drawbacks, such as voids and microcracks. Joule heating due to current crowding around voids or microcracks will cause high local temperature gradient, leading to local non-uniformity in material parameters in the vicinity of voids or microcracks. Local variation in material behaviors could change interconnect life by several orders of magnitude in some conditions[1-6]. Therefore, the effect of the thermomigration driven by temperature gradient should be taken into account in the study of the reliability of interconnect lines. However, little attention has been devoted on the microcrack evolution induced simultaneously by thermomigration, stressmigration and electromigration.

*Corresponding author, E-mail address: pzhuang@nuaa.edu.cn.

How to cite this article: ZHOU Linyong, HUANG Peizhen. Numerical Simulation on Intergranular Microcracks in Interconnect Lines Due to Surface Diffusion Induced by Stress-, Electro- and Thermo-migration[J]. Transactions of Nanjing University of Aeronautics and Astronautics, 2019,36(6):1004-1017.
http://dx.doi.org/10.16356/j.1005-1120.2019.06.013

There have been a number of analytical studies on the grain boundary void growth and the motion of an elliptical inclusion in interconnect lines with bamboo microstructures under stress field, gradient stress field or/and electric field[7-11]. The void morphological evolution induced by electromigration under high current density has also been studied[12-13]. Many theoretical studies indicated that a flat surface under the stress could evolve into a wavy shape via surface diffusion[14-16]. Ru[2-3] analyzed the instability of electromigration induced mass transport in interconnect lines and examined the role of thermomigration caused by electromigration and found that thermomigration is the leading driving force for linear instability.

Experimental observations of damage defects in interconnect lines induced by stressmigration, electromigration and thermomigration have been reported by many workers[1,17-24]. The earlier experiments mainly focused on the void formation, migration, growth in grains or grain boundaries caused by electromigration and the stressmigration. As the temperature effect attracts people's attention widely, Raghavan et al.[21] observed the diffusion of copper through dielectric interconnect line under electric field and elevated temperature and the results showed that both the electric field and the temperature field can strongly affect the lifetime of the dielectric barrier. As for the thermomigration, Du et al.[22] researched the stabilization of the surface morphology of stressed solids using simultaneously applied electric fields and temperature gradients. Tan et al.[23] investigated the effect of temperature and stress gradients on accelerated electromigration test for Cu narrow interconnect lines. Bastawros et al.[24] experimentally studied the electric current induced damage evolution at the crack tip in interconnect lines. And the effect of thermal stress on the electromigration failure time was analyzed by measuring the change of electric resistance during the electromigration test[1].

There are also many numerical analyses on stressmigration and electromigration due to diffusion processes[25-34]. Bower et al.[25-29] showed two dimensional finite element simulations of void evolution due to strain and electromigration induced surface diffusion. Fridline and Kraft simulated the shape changes of voids in bamboo lines induced by stressmigration[30] and electromigration driven[31] surface diffusion. He et al.[32-34] analyzed the intragranular microcracks evolution under surface diffusion induced by stressmigration and electromigration. Du and He et al.[35-36] respectively researched the effect of linewidth on evolution of intergranular and intragranular microcracks in interconnects induced by stressmigration and electromigration. The above works mainly focused on the evolution of voids or microcracks in a grain.

Experimental observations have shown that voids or microcracks often occur on grain boundaries and intergranular microcracks are common sources of failure in bamboo films[37-41]. In addition, intergranular microcracks are likely to grow much more rapidly than those within grains. During service, these microcracks continue to grow and change their shape by stress and electric current driven mass transport, and eventually reach a size that causes an unacceptable increase in the resistance of the line. It is proposed that the intergranular microcrack changes shape due to surface diffusion under the combined action of surface energy, elastic energy, electric current as well as temperature gradient. Thus, there is a great interest in identifying the mechanisms responsible for nucleating and propagating of the intergranular microcracks in interconnect lines, and in finding ways to reduce the likelihood of failure.

In this paper, a model of intergranular microcracks in interconnect line under the stress field, the electric field and the temperature gradient field caused by Joule heating is described. The weak formulation incorporating surface diffusion and evaporation-condensation induced simultaneously by electromigration, stressmigration and thermomigration has not been reported in the literature up to now. The present work extends previous models by accounting in detail for the effects of thermomigration and the grain boundary. The aim of the work is primarily to develop a finite element program to simulate the morphological evolution of the intergranular microcrack under surface diffusion induced simultaneously

by thermomigration, stressmigration and electromigration.

In the next section, an analysis model of two-dimensional intergranular microcrack and the governing equations of surface diffusion are introduced. And then the weak statement is briefly described, which governs the concurrent processes of surface diffusion and evaporation-condensation and a finite element method induced by stressmigration, electromigration and thermomigration is developed. The major focus of the study include the simulation and analysis of the evolution procedure under surface diffusion induced by electromigration, stressmigration and thermomigration. The corresponding effect is discussed in detail. At last the main conclusions are presented.

1 Model and Governing Equations

1.1 Geometric model and boundary conditions

Fig.1 schematically illustrates the cross section of an intergranular microcrack in an interconnect line, which is found in the grain boundary and is symmetrical in shape. The interconnect line is subjected to biaxial tensile stresses $\sigma_x = \sigma_y = \sigma$ and remains elastic. Meanwhile, the interconnect line is subjected to an electric field with a voltage V_0. It is assumed that the distribution of the voltage and the stress in the boundary is uniform and the interconnect line deforms in a state of plain strain and that both the electric and the stress fields in the interconnect line have no component normal to the plane of the figure. Diffusion through the bulk is assumed to be negligible. Therefore, in the absence of grain boundary diffusion, the only mode of mass transport is diffusion along the microcrack surface. We have assumed that the surface energy does not interfere with the electric field, the stress field and the temperature field.

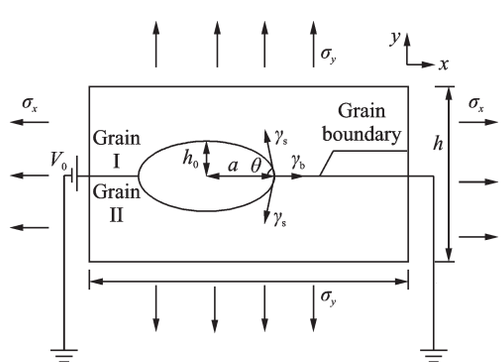

Fig.1 Simplified model of intergranular microcrack in interconnect line under stress and electric fields

For simplicity, the intergranular microcrack is characterized by the aspect ratio $\beta = a/h_0$, where a is the initial major semiaxis of the microcrack, h_0 the initial minor semiaxis, L the length of the interconnect line, and h the linewidth. The surface tension γ_s and the grain boundary tension γ_b must be in equilibrium at the triple point (the microcrack tip) as shown in Fig. 1. This equilibrium requirement leads to a discontinuity in the tangent of free surface at the junction which is often referred to as the dihedral angle 2θ and

$$\cos\theta = \frac{\gamma_b}{2\gamma_s} \tag{1}$$

1.2 Governing equations

The intergranular microcrack changes its shape due to the atom diffusion over its surface. Surface diffusion is driven by the variation in chemical potential, which causes atoms migrate from regions of high chemical potential to those of low chemical potential. Under the effect of the curvature, the stress field and the electric field, the chemical potential μ can be represented as[4]

$$\mu = \mu_0 - Z^* eV - \Omega(\omega - \gamma_s k) \tag{2}$$

where μ_0 is the reference value of μ, Ω the atomic volume, ω the elastic strain energy density, Z^* the effective charge coefficient, V the electric potential, e the charge of an electron and k the curvature of the surface.

Based on Herring's classical theory[42], the atomic flux of the surface diffusion $\boldsymbol{J}$ is proportional to the driving force $\boldsymbol{F}$, which is

$$\boldsymbol{J} = \boldsymbol{M}\boldsymbol{F} \tag{3}$$

where $\boldsymbol{M}$ is the mobility of atoms on the surface and related to the self-diffusivity by the Einstein relation. $\boldsymbol{M} = \Omega D\delta/kT$, in which D is the self-diffusivity on the surface and δ the effective thickness of atoms participating in matter transport. The driving force $\boldsymbol{F}$ is defined by the decrease in free energy per unit volume of matter moving per unit distance on the

surface. The relationship of the driving force and the chemical potential is

$$F=\frac{1}{\Omega^2}\frac{\partial\mu}{\partial s}=\frac{1}{\Omega}\left(\gamma_s\frac{\partial k}{\partial s}-\frac{\partial\omega}{\partial s}\right)-\frac{1}{\Omega^2}Z^*e\frac{\partial V}{\partial s} \tag{4}$$

As the matter is deposited onto or removed from a free surface, the normal velocity v_{ns} of the free surface is generated. According the mass conservation, it is required that

$$v_{ns}=-\nabla\cdot J \tag{5}$$

where $\nabla\cdot J$ stands for the surface divergence of the flux. Let δr_{ns} be the virtual normal displacement on the surface and δI be the virtual mass displacement, we have

$$\delta r_{ns}=-\nabla\cdot(\delta I) \tag{6}$$

For a given system, the chemical potential gradient induces the driving force F. Then through Eqs. (3, 5), the corresponding J and v_{ns} can be obtained, which update the displacement of the point on the intergranular microcrack surface for a small time increment Δt. Repeating the procedure for many time increments, the evolution of the unstable shape for intergranular microcracks can be traced.

2 Formulations of Finite Element Method

2.1 Weak statement for combined surface diffusion and evaporation-condensation

The surface diffusion problem, which conserves solid mass as formulated above, is difficult to implement in a finite element setting. However, once the evaporation-condensation process is introduced into microstructure evolution, the overall mass conservation is easier to treat by the finite element method[43].

Two concurrent processes are imagined to be on a microcrack surface, which include surface diffusion and evaporation-condensation. The kinetic law for evaporation-condensation is similar to that for the surface diffusion. The free energy reduction per unit volume of atoms crossing an interface (denoted by p) is called the driving force on the interface in the evaporation-condensation process and v_{nv} is called the volume of matter added to per unit area of the microcrack surface per unit time. When a structure is not far from the equilibrium, the normal velocity of the interface v_{nv} is proportional to the driving force[44]. The following kinetic law is used.

$$v_{nv}=mp \tag{7}$$

where m is the interface mobility for the evaporation-condensation process.

The resulting equations of the surface normal velocity v_n and the surface virtual displacement δr_n due to the combined action of evaporation-condensation and surface diffusion are

$$v_n=v_{nv}-\nabla\cdot J \tag{8}$$

$$\delta r_n=\delta r_{nv}-\nabla\cdot(\delta I) \tag{9}$$

Associated with the virtual motion, the free energy changes by δG. According to the two kinds of driving forces, F and p, matter relocation and exchange on the microcrack surface area element, δA, reduce the free energy by an amount of $\left(F\cdot\delta I+p\delta r_{nv}\right)\mathrm{d}A$. Thus, the weak formulation for combined surface diffusion and evaporation-condensation can be obtained as

$$\int_A\left(F\cdot\delta I+p\delta r_{nv}\right)\mathrm{d}A=-\delta G \tag{10}$$

Substituting Eqs.(3, 5-9) into Eq.(10) yields

$$\int_A\left\{\frac{J\cdot\delta I}{M}+\frac{\left(v_n+\nabla\cdot J\right)\left(\delta r_n+\nabla\cdot(\delta I)\right)}{m}\right\}\mathrm{d}A=-\delta G \tag{11}$$

The finite element method introduced by Sun et al.[41] is used for solving the above integral equations. The difference between Refs. [32, 33, 43] and this paper is that the coupling with mechanical stress field, temperature gradient field and electric field is considered. That is, the kinetic and mass conservation laws expressed in the left hand side of Eq.(11) are the same, but the energy term in the right hand side of Eq.(11) has three extra terms, including the strain energy from mechanical stress, temperature gradient field, and the electric potential.

2.2 Finite element method

The system consists of two coupled subsys-

tems: the microcrack surface and the solid body. The motion of the microcrack surface is affected by the strain energy induced by the mechanical stress field, the temperature gradient field and the electric potential within the solid body, which in turn is affected by the shape changes due to the surface motion. Each subsystem is discretized into finite elements as follows.

Here, the shape evolution of an elliptical microcrack is studied. Its shape change can be treated as a two-dimensional problem and the microcrack is represented by an area and surface by a curve. Thus, an assembly of linear elements can be used to approach a microcrack surface in two-dimensional problems. Each element has four and three degrees of freedom to describe the motion of element and the diffusion on the element, respectively. These coordinates, together with mass displacement $\boldsymbol{I}$ at all nodal points form generalized coordinates $q_1, q_2, q_3, \cdots, q_{n-2}, q_{n-1}, q_n$, where n is the number of the total degrees of freedom. The generalized velocities are $\dot{q}_1, \dot{q}_2, \dot{q}_3, \cdots, \dot{q}_{n-2}, \dot{q}_{n-1}, \dot{q}_n$. The velocity and virtual motion of any point on the surface can be interpolated by the corresponding values at the nodes. Integrating the weak statement Eq.(11) element by element, a bilinear form in $\dot{q}$ and δq is got. The right-hand side of Eq.(11) is the total free energy change associated with the virtual motion, which is

$$\delta G = -\sum f_i \delta q_i \tag{12}$$

Eq.(12) allows us to compute the generalized forces $f_1, f_2, \cdots, f_n$. Collecting the coefficient of δq_i yields

$$\sum \boldsymbol{H}_{ij} \cdot \dot{q}_j = \boldsymbol{f}_i \tag{13}$$

The free energy variation associated with a given element is computed by

$$\delta G = \gamma_s \delta l - \int_l \omega \delta r_n \, \mathrm{d}s - \int_l \omega^* \delta r_n \, \mathrm{d}s + \frac{Z^* |e|}{\Omega} \int_l V \delta r_n \, \mathrm{d}s \tag{14}$$

where ω^* is the strain energy density caused by temperature gradient stress. The force components acting on the two nodes of the element due to the element surface energy, strain energy density and electric potential are

$$\boldsymbol{f}^e = \gamma_s \begin{bmatrix} \cos\theta \\ \sin\theta \\ 0 \\ -\cos\theta \\ -\sin\theta \\ 0 \\ 0 \end{bmatrix} - \frac{l}{2} \begin{bmatrix} [(2/3)\omega_1 + (1/3)\omega_2]\sin\theta \\ -[(2/3)\omega_1 + (1/3)\omega_2]\cos\theta \\ 0 \\ [(1/3)\omega_1 + (2/3)\omega_2]\sin\theta \\ -[(1/3)\omega_1 + (2/3)\omega_2]\cos\theta \\ 0 \\ 0 \end{bmatrix} - \frac{l}{2} \begin{bmatrix} [(2/3)\omega_1^* + (1/3)\omega_2^*]\sin\theta \\ -[(2/3)\omega_1^* + (1/3)\omega_2^*]\cos\theta \\ 0 \\ [(1/3)\omega_1^* + (2/3)\omega_2^*]\sin\theta \\ -[(1/3)\omega_1^* + (2/3)\omega_2^*]\cos\theta \\ 0 \\ 0 \end{bmatrix} + \frac{Z^* |e| l}{2\Omega} \begin{bmatrix} [(2/3)V_1 + (1/3)V_2]\sin\theta \\ -[(2/3)V_1 + (1/3)V_2]\cos\theta \\ 0 \\ [(1/3)V_1 + (2/3)V_2]\sin\theta \\ -[(1/3)V_1 + (2/3)V_2]\cos\theta \\ 0 \\ 0 \end{bmatrix} \tag{15}$$

where ω_1 and ω_2 represent the strain energy density of nodes 1 and 2, ω_1^* and ω_2^* the strain energy density of nodes 1 and 2 caused by temperature gradient field, and V_1 and V_2 the nodal values of the electric potential function, respectively.

We choose to discretize the solid body and use the standard finite element procedure to solve the electric field, the stress field and the temperature gradient field problem on the current configuration, including the computation of the strain energy density caused by mechanical stress field and temperature gradient field, the electric potential and project the results onto the microcrack surface nodes. Then, the velocity of all the discrete points on the micro-

crack surface is computed by the preceding finite element method under the electric field, stress field and temperature gradient field and let them advance by an amount $v_n\Delta t$ in the direction normal to the surface, where Δt is an appropriately chosen time increment. The simulation of the intergranular microcrack is carried out by repeating the preceding procedures.

3 Numerical Simulation and Discussion

In this section, the behavior of intergranular microcracks caused by surface diffusion induced by stressmigration, electromigration and thermomigration is studied. For convenience, the dimensionless time $\hat{t}=tM\gamma_s/h_0^4$ is introduced in the calculation.

It is known from diffusional theory that the difference in chemical potential constitutes a thermodynamic force, causing atoms to migrate from regions of high potential to those of low potential. The actual evolution of intergranular microcracks in this paper depends on the dimensionless temperature stress and mechanical stress $\hat{\sigma}=\sigma h_0/\gamma_s$, the aspect ratio β and the dimensionless linewidth $\hat{h}=h:h_0$. The relative magnitude of the two forces, the electromigration driving force and the surface tension, is given by $\chi=V_0|e|Z^*h_0/\Omega\gamma_sL$. When the effects of the grain boundary diffusion and evaporation-condensation are neglected, mass conservation requires that the total area of the microcrack during evolution remains constant. In the present study, the actual change of this area during simulation can therefore be taken as a measure of the computing accuracy. As the interface of the microstructure moves, some elements shorten and others elongate. A short element substantially reduces the time step and a very long element poorly models a curved geometry. One minimum and maximum elements are prescribed, a very short element is eliminated, and a very long one is divided. Large numbers of numerical calculations indicate that the finite element method used is robust, accurate and efficient.

3.1 Effect of temperature gradient field

Joule heating due to current crowding around the microcrack will cause high local temperature gradient, leading to local non-uniformity in material parameters in the vicinity of microcracks. In this section, the effect of Joule heating caused by current crowding induced temperature gradient in the vicinity of the evolving microcrack is focused, neglecting the effect of mechanical stress field. The resistivity of the material ρ has a linear temperature dependence[37], which can be expressed as

$$\rho=\rho_0\left[1+\alpha\left(T-T_R\right)\right] \tag{16}$$

where ρ_0 is 1.75 $\mu\Omega\cdot$cm for copper, α the material constant of about 0.004/K at the reference temperature and $T_R=300\,K$ for copper.

Figs.2(a—d) show the evolution of the intergranular microcrack with $\hat{h}=10$, $\beta=4$ for different values of χ=0.2, 0.4, 0.6 and 0.8. In the morphological evolution graphics, the solid lines stand for the results under the electric field and the temperature gradient field, and the dotted lines stand for those only under the electric filed. As shown in Figs.2(e, f), when the current flows through the interconnect line, a temperature gradient field is created inside the conductor, leading to a temperature stress field. It can be seen from Fig.2(e) that the gradient of the temperature field at the microcrack tip is higher than that at the middle of the microcrack, so the corresponding strain energy density ω^* generated by the temperature stress at the microcrack tip is bigger than that at the middle of microcrack. That is, $\omega_A^*>\omega_B^*>\omega_C^*$, as shown in Fig.2(f). The electromigration driving force is proportional to the gradient of the electric potential. It is known that $(\partial V/\partial s)_C>(\partial V/\partial s)_B>(\partial V/\partial s)_A$ in the initial time. Thus, the direction of the electromigration driving force at the right side of the microcrack is the same as that of the thermomigration driving force, which accelerates the microcrack migrating along the electric field direction (see Fig.2(a)). But, the two forces at the left side of the microcrack are in the opposite directions, which are beneficial for the intergranular microcrack to split as shown in Figs.2(b—d). In addition, the intergranu-

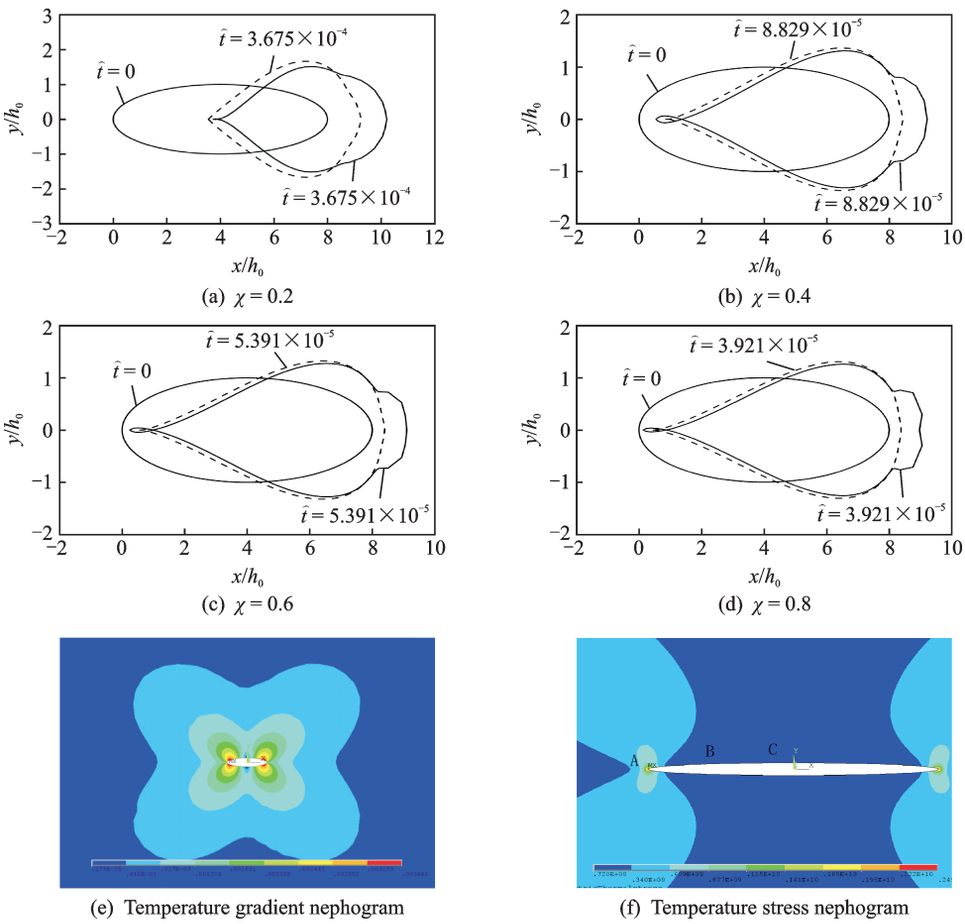

Fig.2 Evolution of intergranular microcrack with $\hat{h}=10$, $\beta=4$

lar microcrack simultaneously grows in linewidth, which tends to accelerate the failure process. The result is consistent with the viewpoint of Ref.[4] and the effect of the thermomigration driven by the temperature gradient should be taken into account in the study. Therefore, in the following numerical simulations, the effect of the temperature gradient field on the evolution of the intergranular microcracks is considered.

3.2 Effect of electric field

Fig.3 shows the evolution of the intergranular microcrack with $\hat{\sigma}=15$, $\beta=4$, $\hat{h}=10$ for different values of $\chi=0.2$, 0.4, 0.6 and 0.8. Here, $\hat{t}_f$ represents the splitting time. As shown in Fig.3(a), the curvature of each point on the microcrack surface is different. The pronounced difference in curvature along the microcrack perimeter induces mass redistribution, with mass being removed from relatively flat microcrack surfaces and depositing in the microcrack tips. The atoms in point C would move to point B, and then move from point B to point A under the electromigration driving force. Moreover, the atoms in point A would move to B and C under the driving force induced by strain energy density. When there is a rest of atoms on point B, a bulge forms. With an increase in the electric field, atoms unceasingly gather on the bulge, while the intergranular microcrack migrates along the interconnect line under the electromigration driving force. When the bulges on the upper and lower surfaces are connected at B' (see Fig.3(b)), the microcrack cavity might split into two small intergranular microcracks. When the bulge reaches a certain size, the atoms will emit from the bulge because the chemical potential here is promoted and is higher than that of the vicinity. If the process takes dominant position, the bulge will revers and eventually the energy in the microcrack surface tends to be the same under surface diffusion as shown in Fig.3(a).

Following the above analysis, there must exist

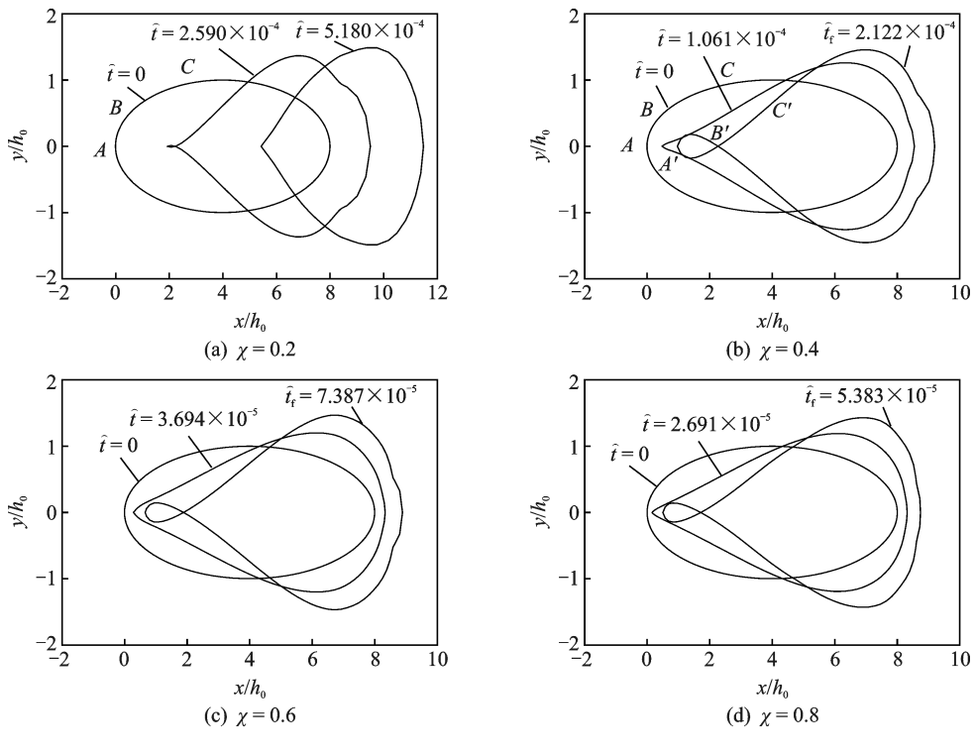

Fig.3 Evolution of intergranular microcrack with $\hat{\sigma}=15$, $\beta=4$, $\hat{h}=10$

a critical electric field χ_c. When $\chi<\chi_c$, the intergranular microcrack will evolve into a stable shape as it migrates along the interconnect line. In contrast, when $\chi\geqslant\chi_c$, the intergranular microcrack splits into two small parts. Fig.4 shows the critical electric field χ_c as a function of the linewidth under different aspect ratios for $\hat{\sigma}=15$. The slope of these curves at any point represents the magnitude of the dependence. It can be seen from the variation tendency of the curve, the critical electric field decreases gradually with the decreases of linewidth, demonstrating that the increasing current density accelerates the microcrack splitting. It also can be found that the larger of the aspect ratio or the electric field, the easier for the intergranular microcrack to split. That is, the increase of the aspect ratio and the electric field are beneficial for the intergranular microcrack to split.

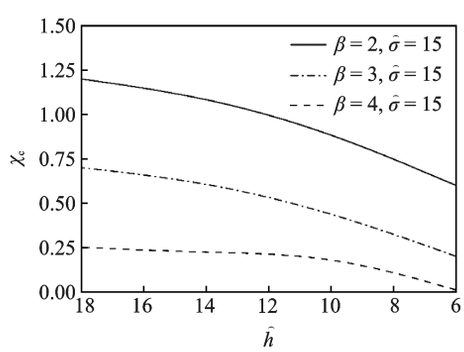

Fig.4 χ_c as a function of the linewidth $\hat{h}$

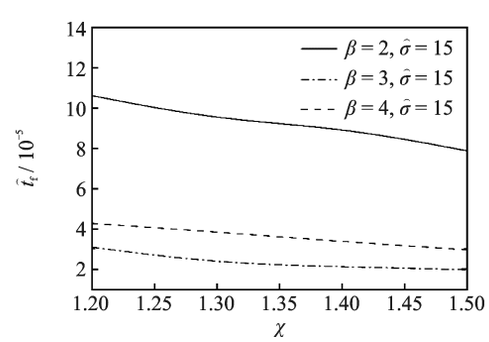

Fig.5 $\hat{t}_f$ as a function of the electric field χ

Fig. 5 shows the relationship of the splitting time $\hat{t}_f$ with χ. It is noticeable that the splitting time decreases as χ increases. This behavior indicates that the increase in χ accelerates the microcrack splitting process. Comparing the curves with different aspect ratios in Fig. 5, it can be seen that the larger of the aspect ratio, the shorter time of the intergranular microcracks needed to split. That is, an increase of the aspect ratio also accelerates the microcrack splitting process.

3.3 Effect of mechanical stress field

Fig. 6 shows the evolution of the intergranular

microcrack with $\chi=0.2$, $\beta=4$, $\hat{h}=10$ for different values of $\hat{\sigma}=15, 20, 25$ and 30. Through the analysis of Fig. 6, it can be concluded that there must exists a critical stress $\hat{\sigma}_c$. When $\hat{\sigma}<\hat{\sigma}_c$, the intergranular microcrack will evolve into a stable shape and migrate along the interconnect line. In contrast, when $\hat{\sigma}\geqslant\hat{\sigma}_c$, the intergranular microcrack will split into two small parts. With the increase of $\hat{\sigma}$, the strain energy density in surface diffusion driving force plays an important role and the left crack tip does not recede and the area of the small part increases (see Figs.6(c) and(d)).

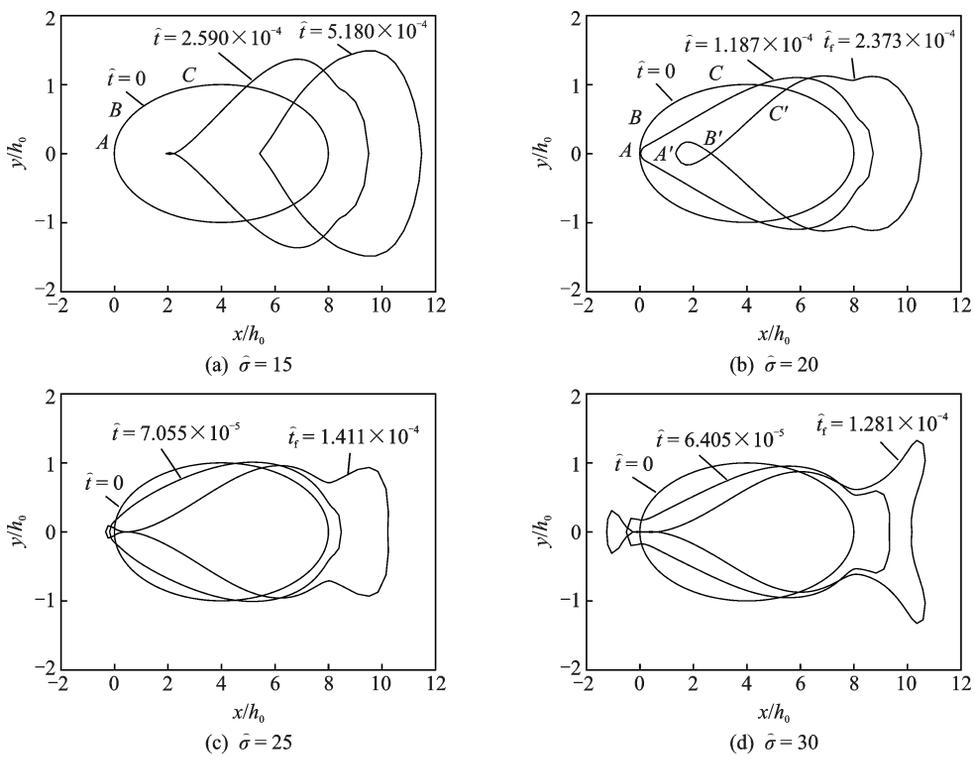

Fig.6 Evolution of intergranular microcrack for $\chi=0.2$, $\beta=4$, $\hat{h}=10$

Fig. 7 shows the critical stress $\hat{\sigma}_c$ of the microcrack splitting as a function of $\hat{h}$. This figure indicates that $\hat{\sigma}_c$ decreases with a decrease of $\hat{h}$ and an increase of the aspect ratio β. It is noticeable that the increase of the aspect ratio β or the decrease of $\hat{h}$ is beneficial to microcrack splitting. In addition, the splitting time decreases as the increases of stress field and aspect ratio for a given electric field, indicating that large values of stress field and aspect ratio accelerate the microcrack split as shown in Fig.8.

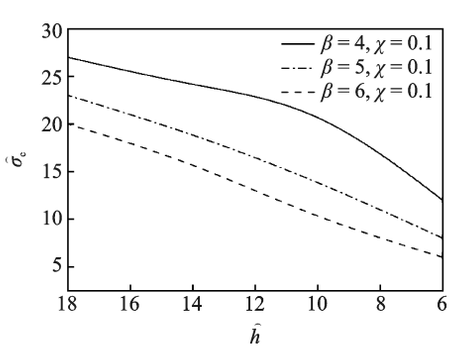

Fig.7 $\hat{\sigma}_c$ as a function of the linewidth $\hat{h}$

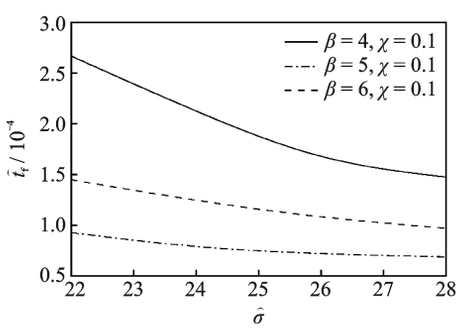

Fig.8 $\hat{t}_f$ as a function of the stress field $\hat{\sigma}$

3.4 Effect of linewidth

Fig. 9 shows the evolution of the intergranular microcrack with $\hat{\sigma}=15$, $\chi=0.2$, $\beta=4$ for the decrease of linewidth ($\hat{h}$=10, 7, 6 and 5). It can be

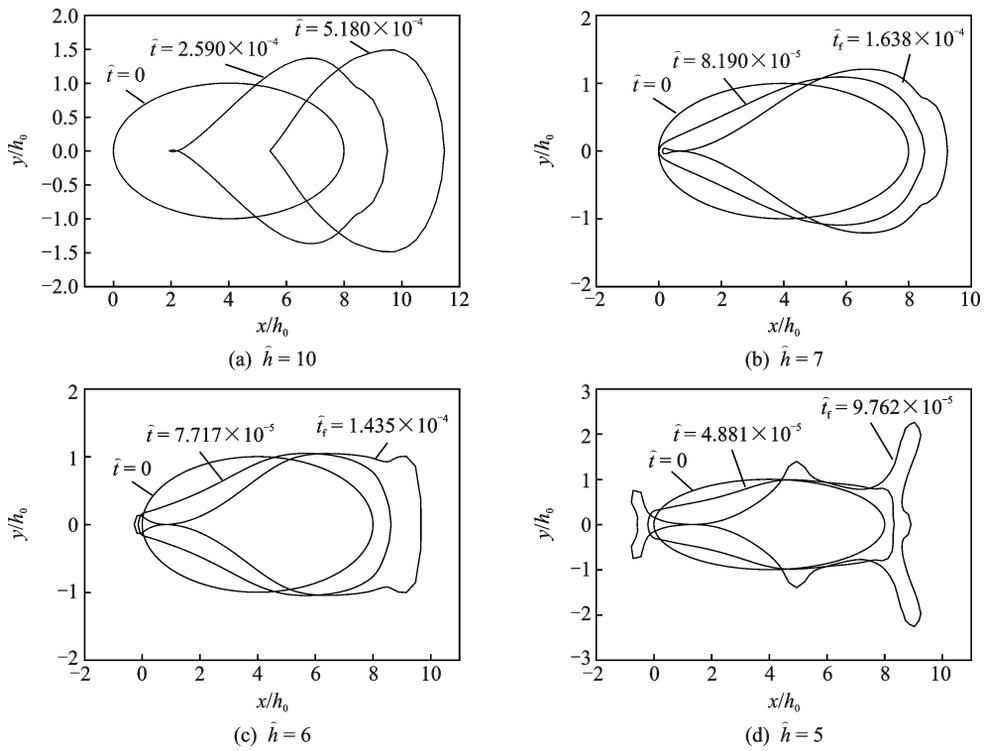

Fig.9 Evolution of the intergranular microcrack for $\hat{\sigma}=15$, $\chi=0.2$, $\beta=4$

seen that there exists a critical linewidth $\hat{h}_c$. When $\hat{h}\leqslant\hat{h}_c$, the microcrack will split into two small parts and with an decrease in linewidth, the morphological evolution is more distinct. Fig.10 reveals the critical linewidth as a function of the electric field. It is noticeable that the critical linewidth increases with an increase in the electric field. When the values of the electric field and the aspect ratio exceed a certain number for a given aspect ratio, the critical linewidth tends to be infinite, which means that the microcrack will split directly. Meanwhile, Fig. 11 shows the splitting time as a function of the linewidth. It can be seen that the splitting time decreases with a decrease in the linewidth for a given electric field, stress field and aspect ratio. That is, reducing the microcrack linewidth can accelerate the microcrack splitting.

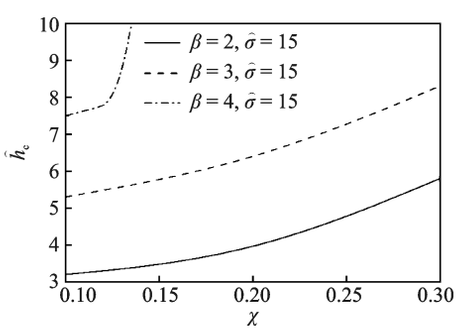

Fig.10 $\hat{h}_c$ as a function of the electric field χ

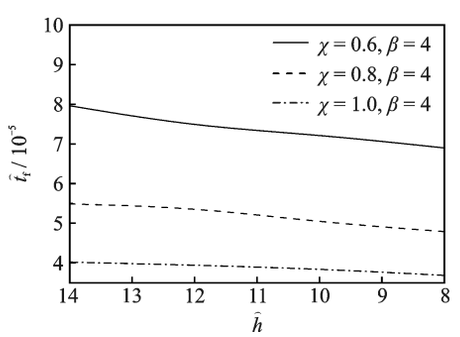

Fig.11 $\hat{t}_f$ as a function of the linewidth $\hat{h}$

3.5 Effect of aspect ratio

Fig.12 shows the evolution of the intergranular microcrack with $\chi=0.2$, $\hat{\sigma}=15$, $\hat{h}=10$ for different values of β=4, 8, 12 and 16. It also can be seen that there exists a critical aspect ratio β_c. When $\beta<\beta_c$, the intergranular microcrack will evolve into a stable shape as it migrates along the interconnect line. When $\beta\geqslant\beta_c$, one or two pair of bulges form on the upper and lower microcrack surface and the intergranular microcrack splits into two or three small parts.

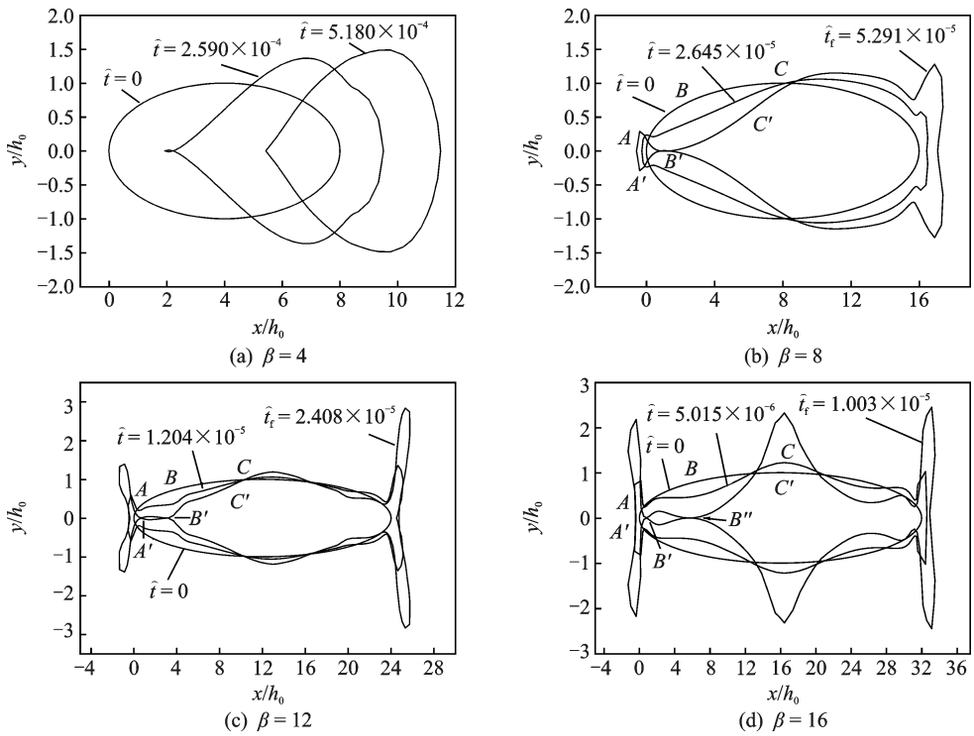

Fig.12 The evolution of the intergranular microcrack for $\hat{\sigma}=15$, $\chi=0.2$, $\hat{h}=10$

Fig.13 reveals the critical aspect ratio as a function of the linewidth. It is noticeable that the critical aspect ratio decreases with the decrease of linewidth. For a given electric field, the microcrack splitting will be much easy to occur with linewidth decreasing. Moreover, the critical aspect ratio β_c decreases with the increase of the electric field, and the increase of the applied electric field is therefore beneficial to microcrack splitting. Fig.14 shows that the splitting time decreases with the increase of the aspect ratio for a given electric field and stress field. The slope of these curves at any point represents the magnitude of the dependence. It can be seen from the variation tendency of the curve, the splitting time dependence of the aspect ratio is relatively

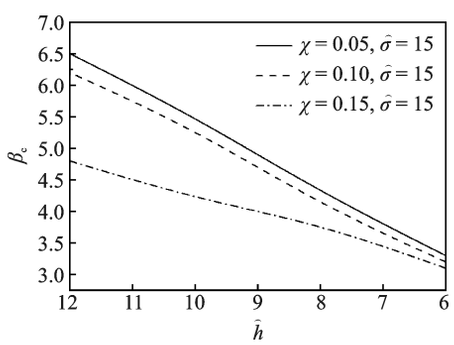

Fig.13 β_c as a function of the linewidth $\hat{h}$

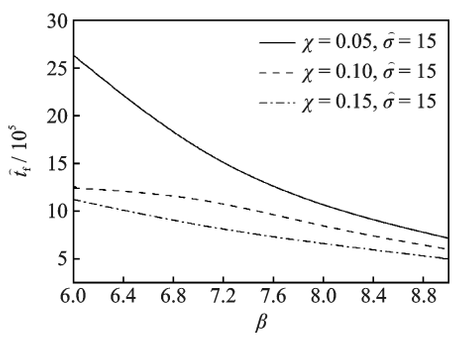

Fig.14 $\hat{t}_f$ as a function of the aspect ratio β

weakened when $\beta\geqslant 8$. Comparing the three curves in Fig.14 respectively, it can be found that the larger of the aspect ratio or the electric field, the faster for the microcrack to split. That is, the increase of the aspect ratio and electric field are beneficial for the microcrack to split.

4 Conclusions

In this paper, the governing equation of the finite element incorporating surface diffusion and evaporation-condensation induced by stressmigration, electromigration and thermomigration is derived and the corresponding program is developed to simulate the morphological evolution of the intergranular microcrack in a copper interconnect line un-

der surface diffusion caused by the mechanical stress field, the electric field and the temperature gradient field. The main results obtained are summarized as follows.

(1) Electromigration induces the temperature gradient field in the vicinity of intergranular microcracks in the interconnect lines, which is beneficial for the intergranular microcrack to split and accelerate the drifting process along the direction of the electric field. The effect of the thermomigration driven by temperature gradient should be taken into account in the evolution of the intergranular microcracks.

(2) There exist a critical electric field χ_c, a critical stress field $\hat{\sigma}_c$, a critical aspect ratio β_c and a critical linewidth $\hat{h}_c$. When $\chi < \chi_c$, $\hat{\sigma} < \hat{\sigma}_c$, $\beta < \beta_c$, $\hat{h} > \hat{h}_c$, the intergranular microcrack will migrates along the interconnect lines stably, and more interesting results show that the microcrack will split into two small parts when $\chi \geqslant \chi_c$, $\hat{\sigma} \geqslant \hat{\sigma}_c$, $\beta \geqslant \beta_c$, $\hat{h} \leqslant \hat{h}_c$. Moreover, with the increase of the aspect ratio, the microcrack even might split into three small parts.

(3) All of χ_c, $\hat{\sigma}_c$, β_c decrease gradually with the decrease of the linewidth. $\hat{h}_c$ increases with the increase of the electric field and the aspect ratio, and tends to be infinite when the value of the electric field and the aspect ratio exceeds a certain value for a given stress field.

(4) The splitting time decreases with the increase of the mechanical stress, the electric field and the aspect ratio, but increases with the increases of the linewidth.

References

[1] LEE S H, KWON D. The analysis of thermal stress effect on electromigration failure time in Al alloy thin-film interconnects[J]. Thin Solid Films, 1999, 341(1/2): 136-139.

[2] RU C Q. Intrinsic instability of electromigration induced mass transport in a two-dimensional conductor [J].Acta Mater, 1999, 47(13): 3571-3578.

[3] RU C Q. Thermomigration as a driving force for instability of electromigration induced mass transport in interconnect lines[J]. Materials Science, 2000, 35(22): 5575-5579.

[4] WANG H, LI Z H, SUN J. Effects of stress and temperature gradients on the evolution of void in metal interconnects driven by electric current and mechanical stress [J]. Modelling and Simulation in Materials Science and Engineering, 2006, 14(4): 607-615.

[5] YU X, WEIDE K. A study of the thermal- electrical- and mechanical influence on degradation in an aluminum-pad structure [J]. Microelectronics and Reliability, 1997, 37(10/11): 1545-1548.

[6] MEINSHAUSEN L, WEIDE-ZAAGE K, FREMONT H. Electro- and thermo-migration induced failure mechanisms in package on package[J]. Microelectronics and Reliability, 2012, 52(12): 2889-906.

[7] SUN Y, LIU M, LU Y, et al. Growth behavior of voids randomly distributed at grain boundary on thin metal film with bamboo microstructures under thermal residual stress field and electric field[J]. Europhysics Letters, 2015, 111(6): 66002.

[8] LI Z H, CHEN N. Electromigration-driven motion of an elliptical inclusion[J]. Applied Physics Letters, 2008, 93(5): 051908.

[9] DONG X, LI Z H. An analytical solution for motion of an elliptical void under gradient stress field[J]. Applied Physics Letters, 2009, 94(7): 071909.

[10] LI Y, LI Z H, WANG X, et. al. Analytical solution for motion of an elliptical inclusion in gradient stress field[J]. Journal of the Mechanics and Physics of Solids, 2010, 58(7): 1001-1010.

[11] CHEN N, LI Z H. WANG X,et al. Grain boundary void growth in bamboo interconnect under thermal residual stress field[J]. Journal of Applied Physics, 2007, 101(3): 033535.

[12] WANG Y, YAO Y. A theoretical analysis of the electromigration-induced void morphological evolution under high current density[J]. Acta Mechanica Sinica, 2017, 33(5): 868-878.

[13] WANG Y, YAO Y. A theoretical analysis to current exponent variation regularity and electromigration-induced failure[J]. Journal of Applied Physics, 2017, 121(6): 065701.

[14] GREKOV M A, KOSTYRKO S A. A film coating on a rough surface of an elastic body[J]. Journal of Applied Mathematics and Mechanics, 2013, 77(1): 79-90.

[15] YANG F, SONG W. Stress-driven morphological instability of axi-symmetrical surface coatings[J]. Inter-

national Journal of Solids and Structures, 2006, 43 (22/23): 6767-6782.

[16] PANAT R, HSIA K J, CAHILL D G. Evolution of surface waviness in thin films via volume and surface diffusion[J]. Journal of Applied Physics, 2005, 97 (1): 013521.

[17] VAIRAGAR A V, MHAISALKAR S G, KRISHNAMOORTHY, et al. Study of electromigration induced void nucleation, growth, and movement in Cu interconnects [C]// 2004 7th International Workshop on Stress-Induced Phenomena in Metallization. Austin, Texas, USA: American Institute of Physics, 2004, 741: 135-147.

[18] VANSTREELS K, CZARNECKI P, KIRIMURA T, et al. In-situ scanning electron microscope observation of electromigration -induced void growth in 30 nm 1/2 pitch Cu interconnect structures[J]. Journal of Applied Physics, 2014, 115(7): 074305.

[19] GENUT M, LI Z, BAUER C L, et al. Characterization of the early stages of electromigration at grain boundary triple junctions[J]. Applied Physics Letters, 1991,58(21): 2354-2356.

[20] ZSCHECH E, HUBNER R, AUBEL O, et al. EM and SM induced degradation dynamics in copper interconnects studied using electron microscopy and X-ray microscopy[C]// 2010 48th Annual IEEE International Reliability Physics Symposium (IRPS). Anaheim, CA, USA: IEEE, 2010: 574-580.

[21] RAGHAVAN G, CHIANG C, ANDERS P B, et al. Diffusion of copper through dielectric films under bias temperature stress[J]. Thin Solid Films, 1995, 262 (1-2): 168-176.

[22] DU L, DASGUPTA D, MAROUDAS D. Stabilization of the surface morphology of stressed solids using simultaneously applied electric fields and thermal gradients[J]. Journal of Applied Physics, 2014, 116(17): 173501.

[23] TAN C M, ROY A. Investigation of the effect of temperature and stress gradients on accelerated EM test for Cu narrow interconnects[J]. Thin Solid Films, 2006,504(1-2): 288-293.

[24] BASTAWROS A F, KIM K S. Experimental study on electric-current induced damage evolution at the crack tip in thin film conductors[J]. Journal of Electronic Packaging, 1998, 120(4): 354-359.

[25] BOWER A F, CRAFT D. Analysis of failure mechanisms in the interconnect lines of microelectronic circuits[J]. Fatigue & Fracture of Engineering Materials & Structure, 1998, 21(5): 611-630.

[26] BOWER A F, FREUND L B. Analysis of stress-induced void growth mechanisms in passivated interconnect lines[J]. Journal of Applied Physics, 1993, 74 (6): 3855-3868.

[27] BOWER A F, SHANKAR S. A finite element model of electromigration induced void nucleation, growth and evolution in interconnects[J]. Modelling and Simulation in Materials Science and Engineering, 2007, 15(8): 923-940.

[28] ZHANG Y W, BOWER A F, XIA L, et al. Three dimensional finite element analysis of the evolution of voids and thin films by strain and electromigration induced surface diffusion[J]. Journal of Mechanics and Physics of Solids, 1999, 47(1): 173-199.

[29] DWYER V M. An investigation of electromigration induced void nucleation time statistics in short copper interconnects[J]. Journal of Applied Physics, 2010, 107 (10): 103718.

[30] FRIDLINE D, BOWER A. Numerical simulations of stress induced void evolution and growth in interconnects[J]. Journal of Applied Physics, 2002, 91(4): 2380-2390.

[31] KRATF O, ARZT E. Numerical simulation of electromigration-induced shape changes of voids in bamboo lines[J]. Applied Physcis Letters, 1995, 66(16): 2063-2065.

[32] HE D, HUANG P Z. A finite-element analysis of intragranular microcracks in metal interconnects due to surface diffusion induced by stress migration[J]. Computational Materials Science, 2014, 87: 65-71.

[33] HE D, HUANG P Z. A finite-element analysis of ingrain microcracks caused by surface diffusion induced by electromigration[J]. International Journal of Solids and Structures, 2015, 62: 248-255.

[34] ZHOU L Y, HUANG P Z, CHENG Q. Effect of interconnect linewidth on the evolution of intragranular microcracks due to surface diffusion in a gradient stress field and an electric field[J]. Journal of Mechanics of Materials and Structures, 2018,13(3): 365-378.

[35] DU Jiefeng, HUANG Peizhen. Effect of linewidth on intergranular microcracks evolution in interconnects [J]. Journal of Nanjing University of Aeronautics & Astronautics, 2017, 49(4): 518-523. (in Chinese)

[36] HE D N, HUANG P Z. Effect of interconnect linewidth on evolution of intragranular microcracks due to electromigration analyzed by finite element method [J]. Transactions of Nanjing University of Aeronau-

tics and Astronautics, 2019, 36(2): 290-297.

[37] ARZT E, KRATF O, NIX W D, et al. Electromigration failure by shape change of voids in bamboo lines [J]. Journal of Applied Physics, 1994, 76(3): 1563-1571.

[38] KRAFT O, BADER S, SANCHEZ J E, et al. Observation and modelling of electromigration -induced void growth in Al-based interconnects[C]// 1993 3th Symposium on Materials Reliability in Microelectronics. San Francisco, CA, USA: Materials Research Society, 1993, 309:199-204.

[39] KRAFT O, ARZT E. Electromigration mechanisms in conductor lines: Void shape changes and slit-like failure[J]. Acta Materialia, 1997, 45(4): 1599-1611.

[40] ROSE J H. Fatal electromigration voids in narrow aluminum-copper interconnect[J]. Applied Physics Letters, 1992, 61(18): 2170-2172.

[41] SANCHEZ J E, MCKNELLY L T, MORRIS J W. Slit morphology of electromigration induced open circuit failures in fine line conductors[J]. Journal of Applied Physics, 1992, 72(7): 3201-3203.

[42] HERRING C. Surface tension as a motivation for sintering, in: The physics of powder metallurgy [M]. New York: McGraw-Hill, 1951: 143-179.

[43] SUN B, SUO Z. A finite element method for simulating interface motion—II. Large shape change due to surface diffusion[J]. Acta Materialia, 1997, 45(12): 4953-4962.

[44] MULLINS W W. Theory of thermal grooving[J]. Journal of Applied Physics, 1957, 28(3): 333-339.

Acknowledgements The work was supported by the Natural Science Foundation of Jiangsu Province of China (No. BK20141407) and the Project Funded by the Priority Academic Program Development of Jiangsu Higher Education Institutions.

Authors Mr. **ZHOU Linyong** received his M.S. degree in Engineering Mechanics from Inner Mongolia University of Science & Technology in 2014. His research has focused on modelling and simulation in materials science and engineering.

Prof. **HUANG Peizhen** received her Ph. D. degree in Solid Mechanics from Xi'an Jiaotong University in 2001. From 2001 to 2003, she was a Postdoctoral Research Fellow in the State Key Laboratory for Mechanical Behavior of Materials, Xi'an Jiaotong University. Since 2003, she has been working at the College of Aerospace Engineering, Nanjing University of Aeronautics and Astronautics. Her research has focused on modelling and simulation in materials science and engineering.

Author contributions Mr. **ZHOU Linyong** contributed to the discussion and analysis as well as prepared all drafts. Prof. **HUANG Peizhen** contributed to the discussion and background of the study.

Competing interests The authors declare no competing interests.

(Production Editor: Wang Jing)